A mixed-space approach to first-principles calculations of phonon frequencies for polar materials

FAST TRACK COMMUNICATION

A mixed-space approach to first-principles calculations of phonon frequencies for polar materials

Y Wang, J J Wang, W Y Wang, Z G Mei, S L Shang, L Q Chen and Z K Liu

Materials Science and Engineering, The Pennsylvania State University, University Park, PA 16802, USA

Abstract

We propose a mixed-space approach using the accurate force constants calculated by the direct approach in real space and the dipole–dipole interactions calculated by linear response theory in reciprocal space, making the accurate prediction of phonon frequencies for polar materials possible using the direct approach as well as linear response theory. As examples, by using the present approach, we predict the first-principles phonon properties of the polar materials α-Al$_2$O$_3$, MgO, c-SiC, and h-BN, which are in excellent agreement with available experimental data.

(Some figures in this article are in colour only in the electronic version)

Currently there are basically two methods in use for the first-principles calculations of phonon frequencies [1–4]: (i) the linear response theory and (ii) the direct approach. Utilizing the approach that the ground-state electron charge density linearly responds to a distortion of the nuclear geometry, the linear response theory directly evaluates the dynamical matrix through the density functional perturbation theory (DFPT) [1, 5] without the approximation of the cutoff in neighboring interactions. Compared with the linear response method, the direct approach is conceptually simple. It adopts the frozen phonon approximation [2, 4] through which the changes in total energy or forces are calculated in real space by displacing the atoms from their equilibrium positions. The advantage of the direct approach is that the phonon frequencies at the exact wavevectors, which are commensurable with the supercell, are calculated exactly with no further approximation [6]. However, all of the current implementations of the direct approach are unable to accurately handle the long range dipole–dipole interactions [7] which result in the well-known LO–TO splitting (splitting between longitudinal and transverse optical phonon frequencies) [1], for the general purpose of calculating phonon density-of-states (PDOS). The dearth of LO–TO splitting in the direct approach

motivates the present work to develop an accurate scheme to incorporate the effects of long range dipole–dipole interactions into the dynamical matrix calculated by the direct approach.

The basic theoretical quantity in lattice dynamics or phonon theory is the reciprocal space dynamical matrix $\tilde{D}_{\alpha\beta}^{jk}(\mathbf{q})$ that is related to the real space force constant $\Phi_{\alpha\beta}^{jk}(0, P)$ by the following Fourier transformation [3]:

$$\tilde{D}_{\alpha\beta}^{jk}(\mathbf{q}) = \frac{1}{\sqrt{\mu_j \mu_k}} \sum_P \Phi_{\alpha\beta}^{jk}(0, P) \exp\{i\mathbf{q} \cdot [\mathbf{R}(P) - \mathbf{R}(0)]\} \tag{1}$$

where $\mathbf{q}$ represents the wavevector, α and β the Cartesian axes of either x, y, or z, j and k the indexes of atoms in the primitive unit cell, μ_j the atomic mass of the jth atom in the primitive unit cell, P the index of the primitive unit cell in the supercell, and $\mathbf{R}(P)$ the position of the Pth primitive unit cell in the supercell.

In general, we can separate the contributions to $\Phi_{\alpha\beta}^{jk}$ in equation (1) into the sum of the short range interactions and the long range interactions as follows:

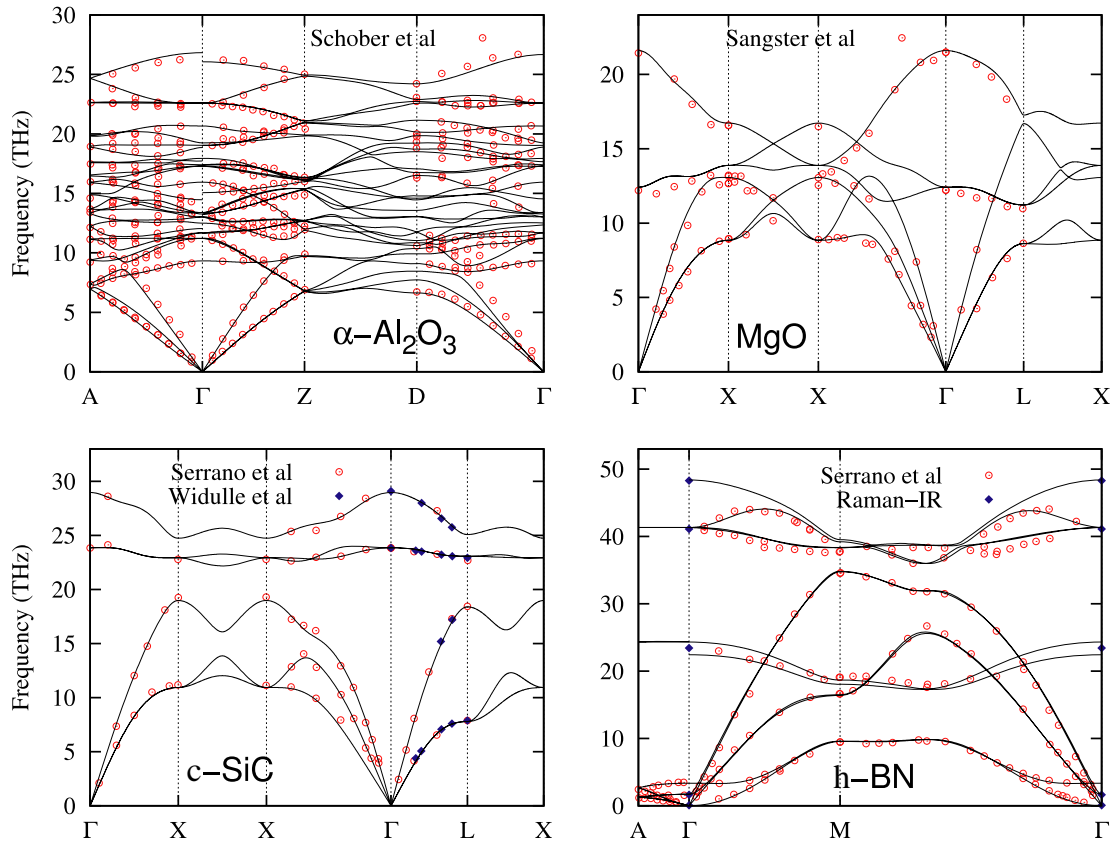$$\Phi_{\alpha\beta}^{jk}(0, P) = \phi_{\alpha\beta}^{jk}(0, P) + \varphi_{\alpha\beta}^{jk} \tag{2}$$

Figure 1. Phonon dispersions of α-Al$_2$O$_3$, MgO, c-SiC, and h-BN. The solid lines represent the present calculations, the open circles (red) are the inelastic neutron scattering or inelastic x-ray scattering data [36–39], and the solid diamonds (blue) are Raman or infrared data [33–35, 48].

where $\phi_{\alpha\beta}^{jk}$ is the contribution from short range interactions, and $\varphi_{\alpha\beta}^{jk}$ the contribution from long range interactions typically due to the dipole–dipole effects. In the linear response theory [1], $\varphi_{\alpha\beta}^{jk}$ is determined by making the inverse Fourier transformation into real space from the calculated dynamical matrix in the limit of zero wavevector. In contrast, as constrained by the periodic condition, the evaluation of $\varphi_{\alpha\beta}^{jk}$ within the direct approach requires the Berry phase approach [6] using special supercells. To calculate the phonon frequencies in the whole Brillouin zone, e.g. aimed at obtaining the accurate PDOS, large numbers of special supercells are needed in the Berry phase approach. Alternatively, Parliński [8] proposed a semi-empirical extrapolation to circumvent this problem, arising in lots of applications (see e.g. [9–25]). Unfortunately, even with the adjustable fitting parameters, Parliński's approach still results in incorrect knots in the phonon dispersion curves (see e.g. [9–25]) in comparison with experiments.

Herein, we find that the long range dipole–dipole interactions, i.e. the contribution of the nonanalytical part to the dynamical matrix, can be accurately incorporated together with the direct approach. According to Cochran and Cowley [26], the nonanalytical part of the dynamical matrix in the limit of zero wavevector is given by

$$\tilde{D}_{\alpha\beta}^{jk}(na) = \frac{4\pi e^2}{V} \frac{[\mathbf{q} \cdot \mathbf{Z}^*(j)]_\alpha [\mathbf{q} \cdot \mathbf{Z}^*(k)]_\beta}{\mathbf{q} \cdot \boldsymbol{\varepsilon}_\infty \cdot \mathbf{q}}, \quad (3)$$

where $\mathbf{Z}^*(j)$ represents the Born effective charge tensor of the jth atom in the primitive unit cell and $\boldsymbol{\varepsilon}_\infty$ the high frequency static dielectric tensor, i.e. the contribution to the dielectric permittivity tensor from the electronic polarization [1].

Since equation (3) is the Fourier transformation of a function in the limit of zero wavevector, we can transform equation (3) back into the zero-order term (in other words, the constant term) of that function. In the case where the function is the force constant in real space, this back transformation gives the zero-order term as

$$\varphi_{\alpha\beta}^{jk} = \frac{\tilde{D}_{\alpha\beta}^{jk}(na)}{N}, \quad (4)$$

where N is the number of primitive cells in the supercell. Note that for the exact wavevectors $\mathbf{q}$, $\mathbf{q} \cdot \mathbf{L}_l = 2\pi n_l$ with $\mathbf{L}_l$ ($l = 1, 2,$ and 3) being the lattice vectors of the supercell and n_l an integer [1, 6]. Important properties associated with equation (4) can be derived using the following equation for the exact wavevectors:

$$\frac{1}{N} \sum_P \exp\{i\mathbf{q} \cdot [\mathbf{R}(P) - \mathbf{R}(0)]\} = \delta(\mathbf{q}), \quad (5)$$

where $\delta(\mathbf{q})$ is zero if $\mathbf{q} \neq 0$ and $\delta(0) = 1$. We observe the following:

(i) at $\mathbf{q} \to 0$, the nonanalytical part of the dynamical matrix in equation (3) is naturally recovered through the summation in equation (1);
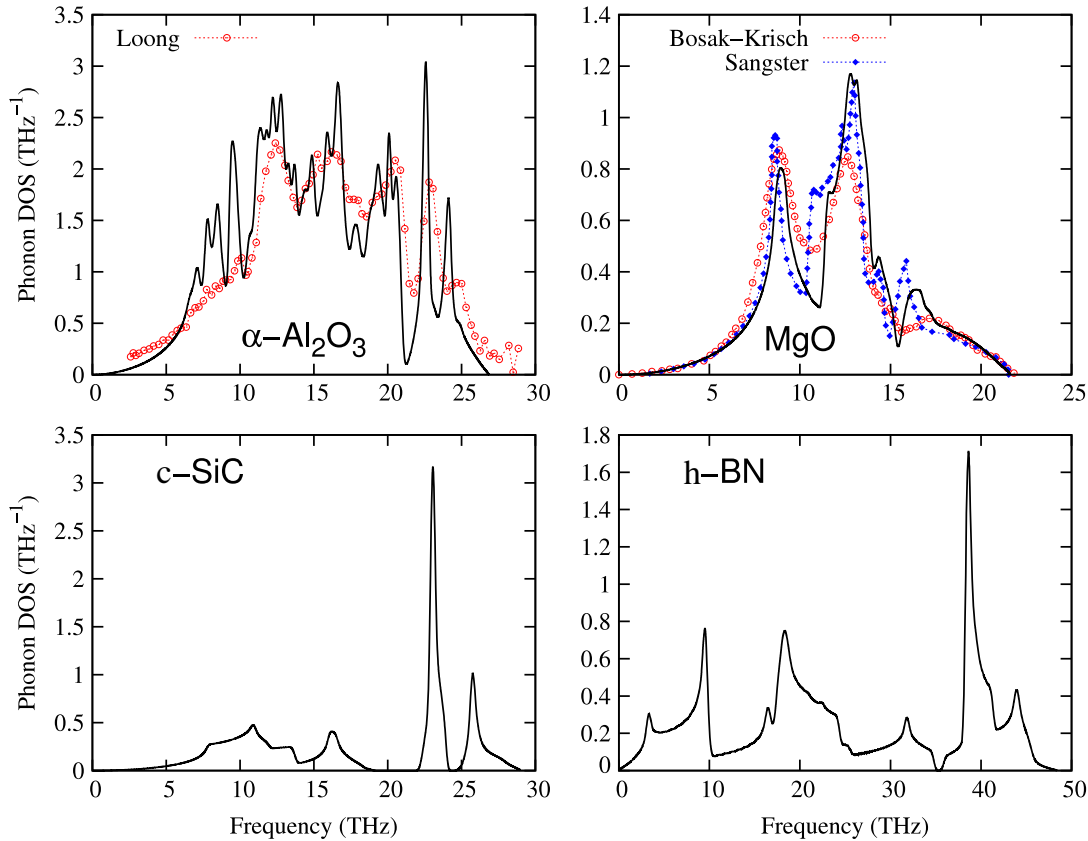
Figure 2. Phonon dispersions of α-Al$_2$O$_3$, MgO, c-SiC, and h-BN. The solid lines represent the present calculations, for α-Al$_2$O$_3$ the open circles (red) connected by the dotted line are the neutron scattering data by Loong [44], for MgO the open circles (red) connected by the dotted line are the inelastic x-ray scattering data by Bosak and Krisch [43], and the solid diamonds (blue) connected by the dotted lines are from the model fitting to their inelastic neutron scattering phonon dispersions for MgO obtained by Sangster *et al* [36].

(ii) at other exact **q** wavevectors, the contribution of the nonanalytical part to the dynamical matrix vanishes through the summation in equation (1); and

(iii) at all other non-exact wavevectors, equation (4) represents an interpolation, being analogous to the linear response theory [1].

We reiterate that the physics of equation (4) lies in the fact that equation (4) is a Fourier transformation back into real space from reciprocal space, since equation (3) is a Fourier transformation of force constants in the limit of zero wavevector. Therefore, as long as the nonanalytical part of the dynamical matrix in equation (3) is calculated using the density functional perturbation theory or the Berry phase approach, one can incorporate the long range dipole–dipole interaction into the direct approach through equation (4) by means of equation (2). This implies that the present approach can make full use of the accuracies of the force constants calculated in real space and the dipole–dipole interactions calculated in reciprocal space.

Accordingly, we avoid the semi-empirical procedure [8, 9, 17] for extrapolating the LO phonon frequencies for a general **q** point between the Brillouin zone center and the zone boundary for polar materials as developed by Parliński [8] for the direct approach. It is worth mentioning that the nonanalytical part of the dynamical matrix is not yet implemented in most phonon

codes, such as the PHON code by Alfe [27] and the ATAT package by van de Walle *et al* [28].

To demonstrate the present approach, we choose the systems possessing rhombohedral, rocksalt, zincblende, and hexagonal symmetries, i.e. α-Al$_2$O$_3$, MgO, c-SiC, and h-BN, respectively, to calculate their phonon dispersions and the PDOSs.

For first-principles static calculations at 0 K, we employed the projector-augmented wave (PAW) method [29, 30] implemented in the Vienna *ab initio* simulation package (VASP, version 5.2). The exchange–correlation functional according to Ceperley and Alder as parameterized by Perdew and Zunger [31] was employed in all calculations. For calculating the static energy, we used the Γ-centered k mesh determined by using over 8000 k points per atom and an energy cutoff of 520 eV. For calculating the Born effective charge tensor and the high frequency static dielectric tensor, we employed the linear response theory implemented in VASP 5.2 by Gajdos *et al* [32] and the same parameter settings as the static calculations. For calculating the force constants in real space, we used the energy cutoff of 400 eV, together with $2 \times 2 \times 2$ supercells (of the primitive cell) and $5 \times 5 \times 5$ k-mesh for α-Al$_2$O$_3$, and $4 \times 4 \times 4$ supercells and $3 \times 3 \times 3$ k-mesh for MgO, c-SiC, and h-BN.

Figure 1 illustrates the calculated phonon dispersions at the theoretical static equilibrium volumes at 0 K by
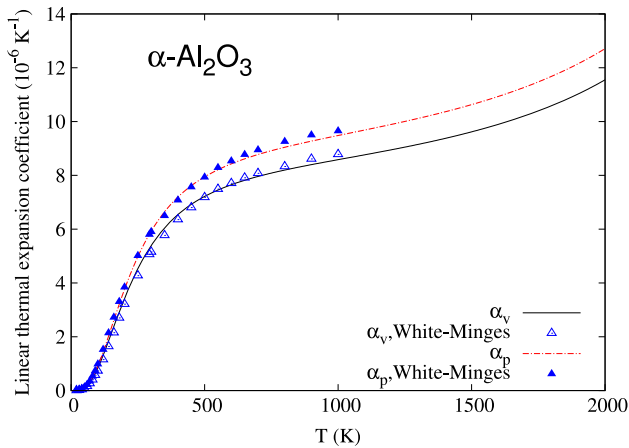
Figure 3. Direction-dependent linear thermal expansion coefficients of α-Al$_2$O$_3$. The solid (black) and dot–dashed (red) lines represent, respectively, the calculated in-plane (α_v, vertical to the rhombohedral axis) and out-of-plane (α_p, parallel to the rhombohedral axis) values. The open and solid triangles (blue) represent, respectively, the in-plane and out-of-plane values critically evaluated by White and Minges [47].
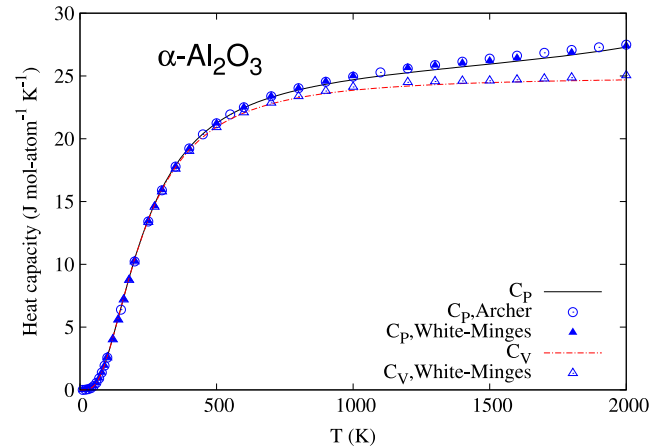

Figure 4. Heat capacities of α-Al$_2$O$_3$. The solid (black) and dot–dashed (red) lines represent, respectively, the calculated isobaric (C_P) and isochoric (C_V) values. The open and solid triangles represent, respectively, the isobaric and isochoric values critically evaluated by White and Minges [47]. The open circles represent the critically evaluated C_P found by Archer [46].

the present approach together with measurements [33–39]. It demonstrates that the present approach has the same accuracies as the linear response theory in predicting the phonon frequencies for α-Al$_2$O$_3$ [40], MgO [41], and c-SiC [42], and the Berry phase approach in calculating the phonon frequencies for h-BN [6]. We can see substantial improvements in the phonon dispersion curves calculated by the present approach over those calculated for α-Al$_2$O$_3$ by Lodziana and Parliński [9].

Figure 2 compares the calculated PDOS obtained by the present approach at the theoretical static equilibrium volumes at 0 K with available measurements [43, 44] or model fitting [36]. The experimental peak positions are overall reproduced. For α-Al$_2$O$_3$ at the low frequency region (<5 THz) we believe the calculation is more reliable. At the high frequency region (>25 THz) for α-Al$_2$O$_3$, the present approach demonstrates the same tendency as that calculated by Heid *et al* [40] using the linear response theory.

As a further application, we predict the thermal expansions, heat capacities, and entropy as a function of temperature up to 2000 K for α-Al$_2$O$_3$ based on the quasiharmonic approach [45], and plot them in figures 3–5, respectively, together with the critically evaluated values according to experiments [46, 47]. It is amazing to note that the present mixed-space approach reproduces excellently the anisotropy of thermal expansion coefficients.

In summary, to calculate the phonon frequencies for polar materials, we propose a parameter-free mixed-space approach which can make full use of the accuracy of the force constants calculated in real space and the dipole–dipole interactions in reciprocal space. The accuracy of the present approach is confirmed by calculating the phonon frequencies of several representative examples: rhombohedral Al$_2$O$_3$, rocksalt MgO, zincblende SiC, and hexagonal BN. We also predicted the thermal properties of α-Al$_2$O$_3$, including the
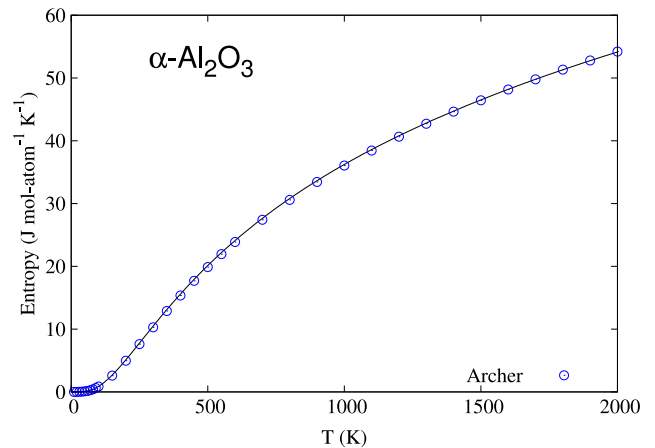

Figure 5. Entropies of α-Al$_2$O$_3$. The solid line represents the present calculation and the open circles represent the critically evaluated values obtained by Archer [46].

direction-dependent thermal expansions, heat capacity, and entropy, as a function of temperature up to 2000 K. We note that our approach does not rely upon existing experimental data or other approximations outside density functional theory (DFT), making the direct approach suitable for accurate predictions of phonon frequencies and related properties of polar materials.

References

[1] Baroni S, de Gironcoli S, Dal Corso A and Giannozzi P 2001 *Rev. Mod. Phys.* **73** 515

[2] van de Walle A and Ceder G 2002 *Rev. Mod. Phys.* **74** 11

[3] Wallace D C 1972 *Thermodynamics of Crystals* (New York: Wiley)

[4] Wei S Q and Chou M Y 1992 *Phys. Rev. Lett.* **69** 2799

[5] Gonze X and Lee C 1997 *Phys. Rev.* B **55** 10355

[6] Kern G, Kresse G and Hafner J 1999 *Phys. Rev.* B **59** 8551

[7] Detraux F, Ghosez P and Gonze X 1998 *Phys. Rev. Lett.* **81** 3297

[8] Parlinski K, Li Z Q and Kawazoe Y 1998 *Phys. Rev. Lett.* **81** 3298

[9] Lodziana Z and Parliński K 2003 *Phys. Rev.* B **67** 174106

[10] Hector L G, Herbst J F and Kresse G 2007 *Phys. Rev.* B **76** 014121

[11] Hu C H, Oganov A R, Wang Y M, Zhou H Y, Lyakhov A and Hafner J 2008 *J. Chem. Phys.* **129** 234105

[12] Wdowik U D and Parlinski K 2008 *Phys. Rev.* B **78** 224114

[13] Derzsi M, Piekarz P, Jochym P T, Lazewski J, Sternik M, Oles A M and Parlinski K 2009 *Phys. Rev.* B **79** 205105

[14] Duan Y H and Sorescu D C 2009 *Phys. Rev.* B **79** 014301

[15] Evarestov R A and Losev M V 2009 *J. Comput. Chem.* **30** 2645

[16] Jiang C, Stanek C R, Marks N A, Sickafus K E and Uberuaga B P 2009 *Phys. Rev.* B **79** 132110

[17] Luo X H, Zhou W, Ushakov S V, Navrotsky A and Demkov A A 2009 *Phys. Rev.* B **80** 134119

[18] Minamoto S, Kato M, Konashi K and Kawazoe Y 2009 *J. Nucl. Mater.* **385** 18

[19] Sevik C and Cagin T 2009 *Phys. Rev.* B **80** 014108

[20] Shi S Q, Ke X Z, Ouyang C Y, Zhang H, Ding H C, Tang Y H, Zhou W W, Li P J, Lei M S and Tang W H 2009 *J. Power Sources* **194** 830

[21] Shi S Q, Zhang H, Ke X Z, Ouyang C Y, Lei M S and Chen L Q 2009 *Phys. Lett.* A **373** 4096

[22] Wdowik U D and Legut D 2009 *J. Phys.: Condens. Matter* **21** 275402

[23] Wdowik U D and Parlinski K 2009 *J. Phys.: Condens. Matter* **21** 125601

[24] Wrobel J, Kurzydlowski K J, Hummer K, Kresse G and Piechota J 2009 *Phys. Rev.* B **80** 155124

[25] Wdowik U D 2010 *J. Phys.: Condens. Matter* **22** 045404

[26] Cochran W and Cowley R A 1962 *J. Phys. Chem. Solids* **23** 447

[27] Alfe D 2009 *Comput. Phys. Commun.* **180** 2622

[28] van de Walle A, Asta M and Ceder G 2002 *CALPHAD* **26** 539

[29] Blöchl P E 1994 *Phys. Rev.* B **50** 17953

[30] Kresse G and Joubert D 1999 *Phys. Rev.* B **59** 1758

[31] Perdew J P and Zunger A 1981 *Phys. Rev.* B **23** 5048

[32] Gajdos M, Hummer K, Kresse G, Furthmuller J and Bechstedt F 2006 *Phys. Rev.* B **73** 045112

[33] Geick R, Perry C H and Rupprech G 1966 *Phys. Rev.* **146** 543

[34] Nemanich R J, Solin S A and Martin R M 1981 *Phys. Rev.* B **23** 6348

[35] Reich S, Ferrari A C, Arenal R, Loiseau A, Bello I and Robertson J 2005 *Phys. Rev.* B **71** 205201

[36] Sangster M J, Peckham G and Saunders Dh 1970 *J. Phys.* C **3** 1026

[37] Schober H, Strauch D and Dorner B 1993 *Z. Phys.* B **92** 273

[38] Serrano J, Bosak A, Arenal R, Krisch M, Watanabe K, Taniguchi T, Kanda H, Rubio A and Wirtz L 2007 *Phys. Rev. Lett.* **98** 095503

[39] Serrano J, Strempfer J, Cardona M, Schwoerer-Bohning M, Requardt H, Lorenzen M, Stojetz B, Pavone P and Choyke W J 2002 *Appl. Phys. Lett.* **80** 4360

[40] Heid R, Strauch D and Bohnen K P 2000 *Phys. Rev.* B **61** 8625

[41] Wang Y, Liu Z K, Chen L Q, Burakovsky L and Ahuja R 2006 *J. Appl. Phys.* **100** 023533

[42] Karch K, Pavone P, Windl W, Schutt O and Strauch D 1994 *Phys. Rev.* B **50** 17054

[43] Bosak A and Krisch M 2005 *Phys. Rev.* B **72** 224305

[44] Loong C K 1999 *J. Eur. Ceram. Soc.* **19** 2241

[45] Wang Y, Liu Z K and Chen L Q 2004 *Acta Mater.* **52** 2665

[46] Archer D G 1993 *J. Phys. Chem. Ref. Data* **22** 1441

[47] White G K and Minges M L 1997 *Int. J. Thermophys.* **18** 1269

[48] Widulle F, Ruf T, Buresch O, Debernardi A and Cardona M 1999 *Phys. Rev. Lett.* **82** 3089